RSC Advances

PAPER

View Article Online
View Journal | View Issue

Cite this: *RSC Adv.*, 2020, **10**, 24169

Antifouling and antimicrobial polyethersulfone/hyperbranched polyester-amide/Ag composite

Ayman El-Gendi,[a] Ahmed F. Ghanem,[b] Mohamed A. Yassin*[bc] and Mona H. Abdel Rehim *[b]

Received 17th April 2020
Accepted 12th June 2020

DOI: 10.1039/d0ra03452e

rsc.li/rsc-advances

This study provided a facile approach for the development of antifouling and antibacterial polyethersulfone (PES) composite film. Mainly, hyperbranched polyester-amide (PESAM) was used as both the reducing and capping agent for the *in situ* formation of AgNPs. The nanoparticles were intensively investigated using Fourier transform infrared spectroscopy (FTIR), ultra-violet spectroscopy (UV-vis), scanning and transmission electron microscopy (SEM & TEM) and X-ray diffraction (XRD). AgNPs were narrowly distributed with an average particle size of about 6 nm. PESAM was mixed with PES to realize free-standing film using the phase inversion method. The inclusion of PESAM in the composite film significantly improved hydrophilicity as confirmed by the contact angle measurements. Furthermore, SEM and EDX investigations confirmed that PESAM induced the *in situ* formation of AgNPs not only on the film surface but also inside its macro-voids. The composite film (PES/PESAM/Ag) displayed significant antibacterial potential against Gram positive and Gram negative bacteria. Overall, the described method paves the way towards development of advanced PES composite films with antimicrobial properties for broad application areas that include desalination membranes or active packaging materials.

1. Introduction

Polyethersulfone (PES) is an amorphous synthetic polymer with distinguishable properties such as transparency, toughness, non-toxicity, sterilizability and high thermal and chemical stability. These remarkable characteristics make PES an ideal polymer for special applications such as medical devices, water desalination membranes and manufacture of baby bottles. However, the hydrophobic nature of PES makes it suffer from biofouling especially in wet applications such as desalination membranes.[1] Therefore, chemical cleaning agents such as chlorine gas or ozone are widely used to remove the accumulated microorganisms on water desalination membranes.[2] Thus, introduction of biocides and improving the hydrophilicity of PES enhance its performance and might extend its applications to new fields. This can be achieved through physical blending of PES with organic and/or inorganic additives. Particularly, many hydrophilic polymers have been reported as additives to improve the antifouling potential of PES including polyvinyl pyrrolidone, polyamide and polyethylene glycol.[3–5] Hyperbranched polymers (HBP) are a special class of polymers that displayed remarkable potential in many applications.[6–8] Indeed, hyperbranched polymers possess irregular branching structure with large number of functional end-groups. In addition, HBP can be easily synthesized in one-pot method which in turn facilitates their commercial production.[9,10] In this context, Mahdavi *et al.* has reported that blending of hyperbranched polyamine ester with PES significantly improved the antifouling potential of membrane. Furthermore, HBP increased the porosity of membrane and induced change in the number and depth of finger like macro-voids leading to reduction of the required pressure for the filtration process.[11] Another study reported that hyperbranched polyamidoamine/polysulfone composite membrane possesses higher water fluxes with potential removal of heavy metal ions from water.[12]

On the other hand, inorganic nanoparticles considered as promising additives that impart additional features on PES composite membrane. To date, many metal and metal oxides nanoparticles such as AgNPs, TiO_2 and ZnO are reported as antimicrobial additives for PES.[13–15] Particularly, it is well known that silver nanoparticles possess high biocidal effect against 16 species of bacteria.[16] This makes silver an excellent antibacterial agent in many sectors including textile, medical, water and food packaging.[17] Currently, AgNPs can be synthesized using variety of methods, such chemical, physical, electrochemical, sonochemical and biological methods.[16] However, chemical reduction of silver salt to generate AgNPs is a simple one-step process. Moreover, different shapes of AgNPs can be obtained by controlling reduction rate and capping agent.[18]

[a]*Chemical Engineering and Pilot Plant Department, Engineering Division, National Research Centre, Giza, Egypt*

[b]*Packaging Materials Department, Chemical Industries Research Division, National Research Centre, Giza, Egypt. E-mail: monaabdelrehim23@gmail.com*

[c]*Advanced Materials and Nanotechnology Lab., Center of Excellence, National Research Centre, Giza, Egypt. E-mail: yassin@daad-alumni.de*

Hyperbranched polymer is one of the efficient stabilizing agents of AgNPs since it possesses large number of functional end-groups. Carboxyl-terminated hyperbranched polyester has been used to stabilize AgNPs in aqueous medium for inkjet printing of flexible circuits.[19] However, hyperbranched polymer containing tertiary amino groups displayed dual function with AgNPs. Mainly, besides its role as stabilizing agent, it acts as reductant due to the reducing power of tertiary amino groups which induced the *in situ* reduction of silver ions.[20] In this context, hyperbranched polyethylenimine and hyperbranched polyamidoamine have been reported for the *in situ* formation of antimicrobial colloidal silver nanoparticles.[21,22]

In this work, hyperbranched polyester-amide (PESAM) based on phthalic anhydride and diisopropanolamine was evaluated as self-reducing and capping agent for *in situ* formation of AgNPs nanohybrid. In addition, a composite film of PES and hyperbranched PESAM was developed using phase inversion method. From one side, PESAM enhanced the hydrophilicity of membrane. From other side PESAM induced the *in situ* formation of antimicrobial AgNPs on both the surface and pores of membrane. The antimicrobial potential of the composite membrane in addition to the morphology of bacteria on the surface of membrane were investigated.

2. Experimental

2.1. Materials

Phthalic anhydride (Ph-An; 99%) and diisopropanolamine (DIPA; 98%) were purchased from Fluka, Germany. Silver nitrate ($AgNO_3$; 99%) and *N*-methyl-2-pyrrolidone (NMP) were purchased from Sigma-Aldrich, Germany. Polyethersulfone (PES; M_n 49 000 g mol^{-1}) was supplied by BASF, Germany. Other chemicals were of analytical grade.

2.2. Characterization

UV-visible characterization of AgNPs was carried out using JASCO V-630 spectrophotometer. Fourier Transform Infrared Spectroscopy (FTIR) investigations were conducted using PerkinElmer. X-ray diffraction analysis was carried out using Bruker diffractometer (Bruker D8 advance target). CuKα radiation source with secondly monochromator ($\lambda = 1.5405$ Å) at 40 kV and 40 mA was used with a scanning rate 0.2 min^{-1}. The molecular weight of the PESAM was determined using Gel Permeation Chromatography technique (GPC) from Agilant. The instrument is connected with refractive index detector and dimethyl formamide (DMF) was used as eluent with 1 ml min^{-1} flow rate. The morphology of the prepared PESAM/Ag nanohybrid was examined using Transmission Electron Microscope (TEM), JEOL JEM-1230, with acceleration voltage of about 80 kV. Contact angel measurements were carried out by captive bubble method based on Axisymmetric Drop Shape Analysis Profile (ADSA-P). Surface and cross-section morphology of pristine and composite PES films were examined using SEM (JEOL). Cross-sectional samples were prepared with wet quick-frozen technique using a Leica UC7 ultramicrotome at −120 °C then samples were sputtered with 3 nm of platinum. Bacterial samples were fixed with 2.5% glutaraldehyde, then the fixed bacteria was dehydrated in graded ethanol series (30, 50, 75, 90, 95 and 100% v/v). Afterward, samples were sputter-coated with thin gold layers for observation by SEM. Energy-dispersive X-ray spectroscopy (EDX) measurements were conducted to display the presence of silver on the composite film.

2.3. Synthesis of hyperbranched polyester amide (PESAM)

PESAM was synthesized using our previously described protocol with slight modification.[23] Briefly, Ph-An (0.17 moles) was reacted with D1PA (0.23 moles) under inert atmosphere at 140 °C for 3 h. After complete dissolution of Ph-An, vacuum was applied for further 2 h to remove water. The reaction was stopped when the color of mixture was turned into yellowish viscous liquid. The prepared polymer is soluble in water, methanol and high polar solvents. The yield was around 87%.

2.4. Preparation of PESAM/Ag nanohybrid

Fresh solution of silver nitrate (0.1 g/2 ml water) was prepared and covered with aluminum foil. Then, a solution of PESAM (1 g/8 ml water) was added slowly and stirred at room temperature for 24 h. A brownish colloidal solution of PESAM/Ag nanohybrid was obtained.

2.5. Preparation of polyethersulfone/hyperbranched polyester amide film (PES/PESAM)

PES/PESAM film was prepared by phase inversion method.[24] Particularly, equal weight ratio of the synthesized PESAM and PES were dissolved in NMP as a solvent. The polymer: solvent ratio was 20 : 80 and the polymers solution was left for 24 h under vigorous stirring. The homogeneous blend solution was degassed under vacuum and casted on a clean glass substrate using blade casting knife of 100 μm thickness. The glass substrate was immersed a coagulation bath (water) for 60 min. at 25 °C. Finally, the prepared free standing film was rinsed with deionized water and left on stand for drying.

2.6. Preparation of composite film (PES/PESAM/Ag)

PES/PESAM blend film was decorated with silver nanoparticles *via in situ* reduction. Particularly, 2 × 2 cm^2 area of PES/PESAM film was immersed in a solution of 1% $AgNO_3$ for 72 h. Then, solution of PESAM (10% w/v) was added and left under mild stirring for 24 h. The composite film was removed, washed well and dried overnight on stand.

2.7. Antimicrobial activity test

Antibacterial experiments were conducted using both Gram-positive *Staphylococcus aureus* (*S. aureus*) and Gram-negative *Escherichia coli* (*E. coli*). The antimicrobial potential of blank PES film and composite film (PES/PESAM/Ag) were evaluated using agar diffusion method. Particularly, both bacterial species were individually inoculated on solid agar plates then film samples (1 × 1 cm) were placed on thin layer of bacteria. The plates were incubated at 37 °C for 24 h and the inhibition zones were measured and digitally photographed.

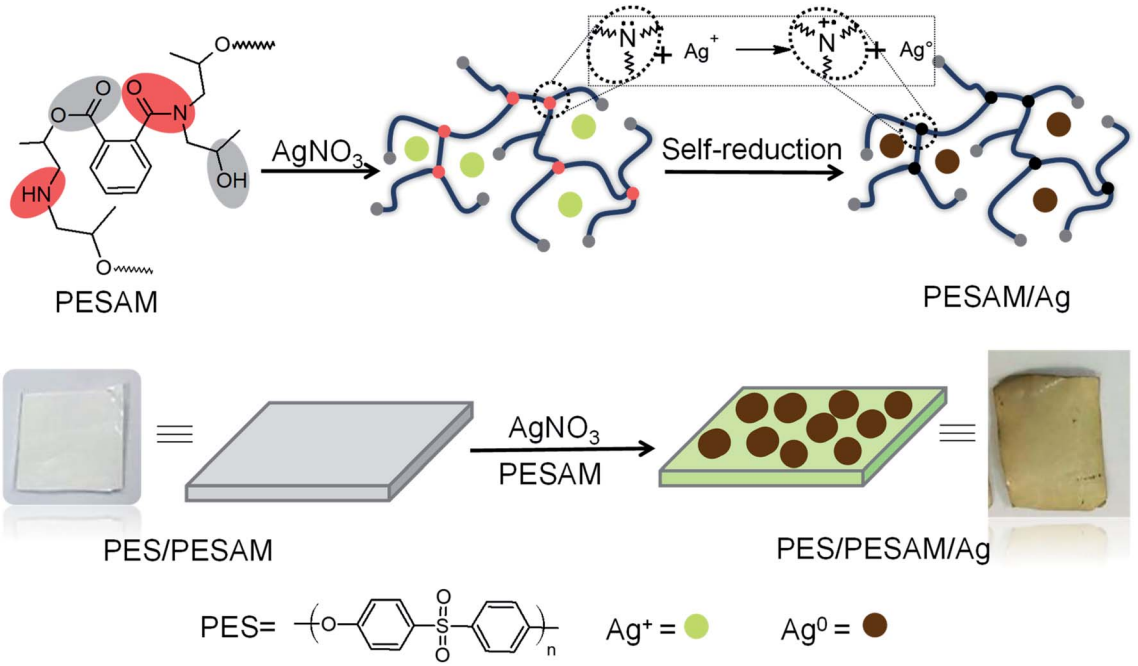

Scheme 1 Schematic representation of PESAM/Ag nanohybrid and composite film (PES/PESAM/Ag) preparation.

To evaluate the antifouling potential, blank PES film and composite film (PES/PESAM/Ag) were incubated in bacteria suspension for 24 h then films were gently rinsed with water. The adhered bacteria were fixed, sputtered with gold and inspected by scanning electron microscope.[25]

3. Results and discussion

3.1. Formation of PESAM/Ag nanohybrid

Aromatic hyperbranched polyester amide (PESAM) was synthesized *via* polycondensation of phthalic anhydride and diisopropanolamine. The realized hyperbranched polymer is water soluble and has M_n value of about 11 000 g mol^{-1}. As shown in Scheme 1, PESAM possesses large number of hydroxyl, ester, tertiary amide and secondary amine groups that can play a crucial role in the *in situ* formation and stabilization of silver nanoparticles. Particularly, by adding a solution of $AgNO_3$ to PESAM solution, the color was gradually changed to brown indicating the *in situ* formation of AgNPs. Such observation was confirmed by UV-visible absorption spectra of both pure PESAM and PESAM/Ag nanohybrid as shown in Fig. 1. The pure PESAM displayed no peak above 300 nm. However, the PESAM/Ag nanohybrid spectrum revealed a new absorption band at around 412 nm which is characteristic for surface plasmon resonance of silver nanoparticles.[26]

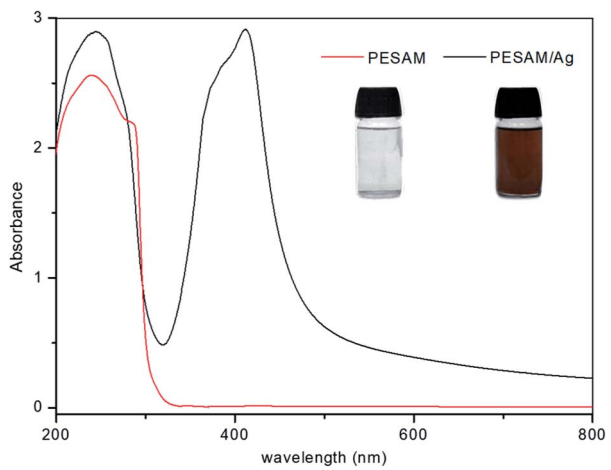

Fig. 1 UV-vis spectra of PESAM solution and PESAM/Ag nanohybrid (insets are their digital images).

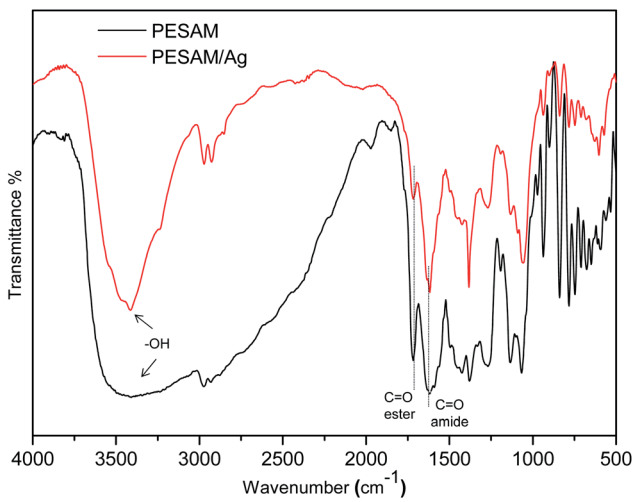

Fig. 2 FTIR spectra of PESAM/Ag nanohybrid and pure PESAM.

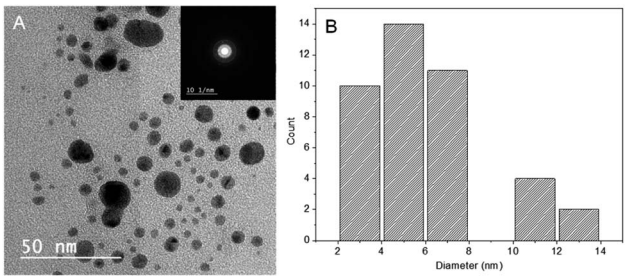

Fig. 3 (A) TEM micrograph of PESAM/Ag nanohybrid (inset is the electron diffraction) and (B) histogram for particle size distribution.

The potential of PESAM as a self-reducing agent to produce AgNPs can be attributed to the plenty of hydroxyl and ester groups in PESAM that can act as anchors for adsorption and complexation with Ag^{+}.[27] Such silver ions were eventually *in situ* reduced into Ag^{0} by means of the strong reducing ability of tertiary amide and secondary amine groups in PESAM. Indeed, similar reducing potential was reported by Zhang *et al.* who confirmed that nitrogen atom in the 1°, 2° and 3° amine of hyperbranched polymer can pass one of its lone pair of electron to Ag^{+} leading to formation of zero-valent silver atoms that spontaneously aggregate together to form AgNPs (Scheme 1).[20,21] Actually, PESAM not only induced the *in situ* reduction of silver ions, but also stabilized the formed AgNPs due to the interactions of the hydroxyl and carbonyl groups with the metallic silver nanoparticles. Fig. 2 displayed the FTIR spectrum of the PESAM/Ag nanohybrid compared with neat PESAM. The spectrum of PESAM/Ag nanohybrid displayed the characteristic bands of PESAM groups that can interact with AgNPs were clearly observed. Particularly, the intense band at 3424 cm^{-1} is attributed to the –OH groups. The stretching vibration band of amide (C=O) was recorded at 1625 cm^{-1}. However the absorption bands of ester were observed at 1720 cm^{-1} (ester C=O stretching) and at 1380 cm^{-1} & 1065 cm^{-1} (asymmetrical and symmetrical C–O–C stretching, respectively).[28] By

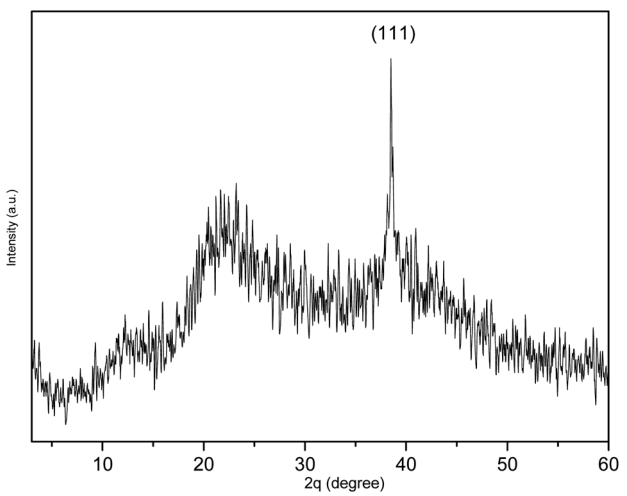

Fig. 4 XRD spectrum of PESAM/Ag nanohybrid.

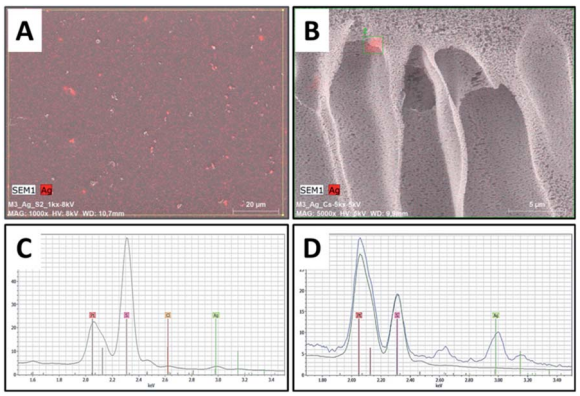

Fig. 5 SEM images of PES/PESAM/Ag composite film, (A) top surface, (B) cross section image, (C and D) EDX spectra of top and cross-sectional images, respectively.

comparing the two spectra, the characteristic bands were tiny shifted but the band sharpness of PESAM/Ag nanohybrid was significantly improved. Particularly, the broadening of –OH band at 3424 cm^{-1} in the pure PESAM was decreased to large extent in the nanohybrid spectrum. These changes indicated the rupture of the intermolecular hydrogen bonding network due to formation of coordination between silver nanoparticles and PESAM surface groups'. It should be noted that the low intermolecular chain entanglement of the hyperbranched PESAM significantly enhanced the dispersion of nanoparticles.

As shown in Fig. 3A, the TEM image of PESAM/Ag nanohybrid revealed that the formed AgNPS are spherical and well dispersed. This confirmed the potential of PESAM to stabilize AgNPs through confining them in the free space within polymer branches. The histogram presented in Fig. 3B showed that the average particle size of PESAM/Ag nanohybrid was about 6 nm. The particles sizes were narrow distributed in the range of 3–7 nm. Indeed, few bigger particles were observed in the range of 10–14 nm due to aggregation, however, these sizes still small (Fig. 3B). Therefore, the solution of PESAM/Ag nanohybrid remained stable over several weeks without observed precipitation. The electron diffraction of the obtained silver nanoparticles displayed highly polycrystalline structure (Fig. 3A, inset). Furthermore, the XRD pattern of

Table 1 Inhibition zone of PES/PESAM/Ag composite film and blank PES film against different bacteria strains after incubation at 37 °C for 24 h

		Inhibition zone (mm)	
Microorganism	Type	Composite film	Blank film
Bacillus cereus	Positive	17	No zone
Staphylococcus aureus	Positive	25	
Pseudomonas aeruginosa	Negative	15	
Escherichia coli	Negative	18	
Candida albicans	Yeast	12	

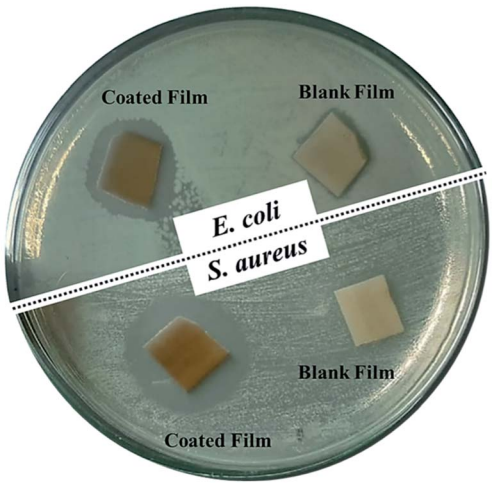

Fig. 6 Digital images of inhibition zone assay of PES/PESAM/Ag composite film and blank PES against two bacteria strains after incubation at 37 °C for 24 h.

PESAM/Ag nanohybrid showed a sharp crystalline diffraction peak at 38° corresponding to (111) plane of AgNPs.[21] A broad non-crystalline peak (18–25°) was also recognized implying the amorphous nature of the hyperbranched polymer (Fig. 4).[29]

3.2. Formation of PES/PESAM/Ag composite film

Hydrophobicity of polyethersulfone (PES) is one of its main disadvantages which allows the colonization of bacteria on its surface leading to biofilm formation especially in wet applications.[1] Therefore, the potential of PESAM to *in situ* formation of AgNPs has been directed to the development of antimicrobial composite film based on PES and PESAM/Ag nanohybrid. Particularly, PESAM was mixed with PES then a blend film was prepared by phase inversion technique in water as coagulant. Despite the hydrophilic nature of PESAM, it was well mixed with PES during film formation. This can be attributed to the π–π interactions between the aromatic rings of PESAM and PES this in addition to the presence of hydrogen bonding between SO_2 groups of PES and OH groups of PESAM which improved the compatibility.[11] Indeed, presence of PESAM in the blend film (PES/PESAM) increased the hydrophilicity of the blend film which in turn enhances its antifouling property. This was confirmed by contact angle measurements which showed that advance contact angle (θ_a°) of blank PES was 70°, however the contact angle of blend film (PES/PESAM) was decreased to 58°. By incubation of the blend film (PES/PESAM) in a solution of $AgNO_3$ and PESAM, both of free and imbedded PESAM will synergistically promote the *in situ* formation of AgNPs not only on the surface of film but also inside the cavities of film. The contact angle of the resulted composite film was further decreased to 34° indicating the enhancement of surface hydrophilicity.

Surface and cross-sectional morphology of the composite film (PES/PESAM/Ag) was studied by SEM (Fig. 5). Generally, a typical morphology of PES membrane was observed with a porous skin layer and finger-like macro-voids in the sub-layer.[30] Images represented in Fig. 5A and B confirmed that homogenous AgNPs (labeled in red color) were successfully formed not only on the surface but also inside the macro-voids of film. This indicated that using the *in situ* formation approach enabled the formation of AgNPs in the macro-voids of film. Furthermore, EDX investigations revealed peak at about 3 keV corresponding to silver (Fig. 5C and D).

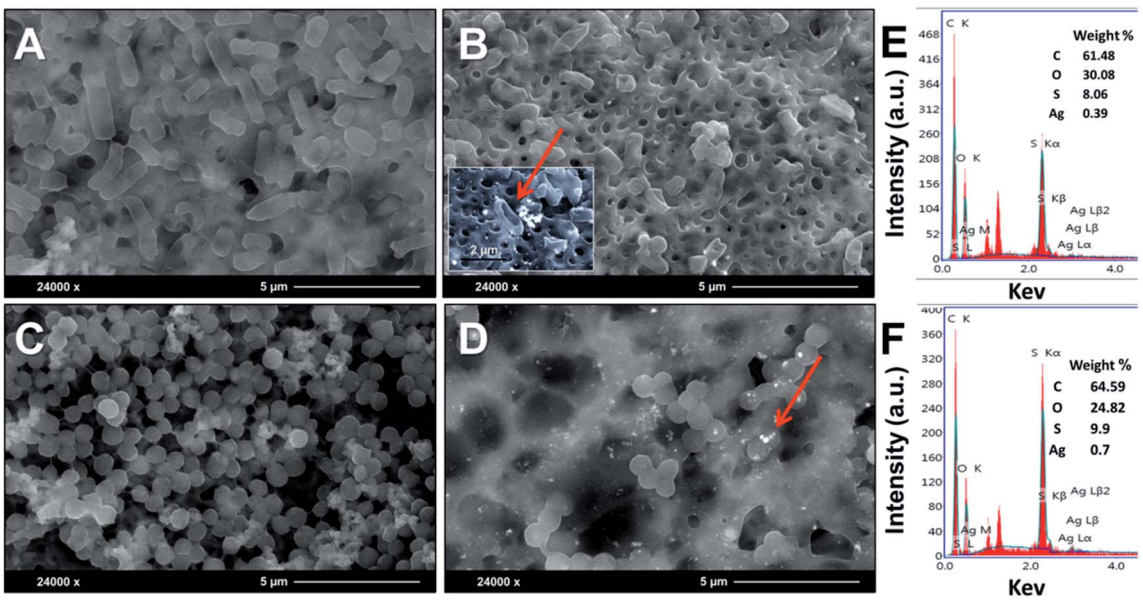

Fig. 7 SEM micrographs of *E. coli* and *S. aureus* grown on the tested surfaces for 24 h. (A and B) Blank PES and composite film (PES/PESAM/Ag) against *E. coli*, respectively. (C and D) Pure PES and composite film (PES/PESAM/Ag) against *S. aureus*, respectively. (E and F) EDX spectra of scanned spots represented by red arrows.

The antimicrobial potential of the composite film (PES/PESAM/Ag) was investigated against different Gram-positive and Gram-negative bacterial strains (Table 1). Overall, the blank PES film displayed no inhibition zone. However, the composite film (PES/PESAM/Ag) displayed a broad inhibition zone against different Gram-positive and Gram-negative strains. For instance, the composite film displayed inhibition zone with diameter of about 18 mm against *E. coli* while, the diameter of inhibition zone was 25 mm in case of *S. aureus* (Fig. 6). These findings indicated that the developed composite film possesses significant antibacterial potential when compared with the PES/PEI/Ag composite film reported by Khona *et al.* that displayed inhibition zone of about 10 mm against *S. aureus.*[22] The biocidal potential of (PES/PESAM/Ag) composite is derived from AgNPs. One of the well-known mechanisms is the oxidation of AgNPs to silver ions that released from the film and interact with the thiol groups in protein and enzymes found on the cellular surface, leading to protein deactivation and bacterial death.[25,31]

SEM investigation was conducted to study the morphology and adherence of both bacterial strains on the surface of blank PES and composite film (PES/PESAM/Ag). Fig. 7A and C illustrated that the surface of blank PES was covered with intact bacteria colonies. The hydrophobic nature of the PES makes its surface favorable for bacteria adhesion and proliferation. However, Fig. 7B and D showed that number of bacteria was significantly reduced on the surface of (PES/PESAM/Ag). The few observed bacterial showed irregular morphology and rougher surface. This due to the biocidal potential of AgNPs which interact with the cell membrane of bacteria leading to rupture of cell membrane and subsequently leakage of the cytosolic components (Fig. 7B inset). This was further confirmed by EDX investigation recorded on the surface of both bacteria strains. Spectra depicted in Fig. 7E and F displayed presence of silver peak on the surface of bacteria which confirmed the involvement of Ag species in the deformation of bacteria cell. It should be noted that presence of PESAM in the (PES/PESAM/Ag) imparted anti-fouling feature on the film due to increasing the hydrophilicity as previously confirmed which in turn enhanced detach of bacteria form the surface.

4. Conclusions

Hyperbranched polyester-amide (PESAM) was employed as both reducing and capping agent for the *in situ* formation of PESAM/Ag nanohybrid. The realized nanohybrid was investigated by UV-vis, FTIR, XRD and TEM. AgNPs were narrow distributed with average particle size of about 6 nm. In addition, PESAM was mixed with polyethersulfone (PES) to realize free standing blend membrane using phase inversion method. Contact angle measurement revealed that the hydrophilicity of the blend film was significantly improved due to the hydrophilic nature of PESAM. Furthermore, PESAM induced the *in situ* formation of AgNPs not only on film surface but also inside its macro-voids. Moreover, agar diffusion test and morphology of bacteria inspected by SEM clearly displayed the bactericidal potential of PES/PESAM/Ag composite film against Gram positive and Gram negative bacteria. Generally, modification of PES with PESAM could be a promising and facile approach for the establishment of antifouling and antibacterial PES composite film. Indeed, PESAM not only enhances the antifouling property due to its hydrophilic nature but also provides antimicrobial feature by inducing *in situ* formation of AgNPs.

Conflicts of interest

There are no conflicts to declare.

Acknowledgements

Authors greatly acknowledge Dr K. Grundke at Institute for Polymer Research Dresden, Germany for contact angle measurements.

References

1 T. A. Otitoju, A. L. Ahmad and B. S. Ooi, *RSC Adv.*, 2018, **8**, 22710–22728.
2 T. Nguyen, F. A. Roddick and L. Fan, *Membranes*, 2012, **2**, 804–840.
3 J. Garcia-Ivars, M.-I. Alcaina-Miranda, M.-I. Iborra-Clar, J.-A. Mendoza-Roca and L. Pastor-Alcañiz, *Sep. Purif. Technol.*, 2014, **128**, 45–57.
4 A. Sumisha, G. Arthanareeswaran, Y. L. Thuyavan, A. Ismail and S. Chakraborty, *Ecotoxicol. Environ. Saf.*, 2015, **121**, 174–179.
5 A. Shockravi, V. Vatanpour, Z. Najjar, S. Bahadori and A. Javadi, *Microporous Mesoporous Mater.*, 2017, **246**, 24–36.
6 M. A. Yassin, A. A. M. Gad, A. F. Ghanem and M. H. A. Rehim, *Carbohydr. Polym.*, 2019, **205**, 255–260.
7 D. Dzema, L. Kartsova, D. Kapizova, S. Tripp, N. Polikarpov, D. Appelhans and B. Voit, *JPC (J. Planar Chromatogr.) - Mod. TLC*, 2016, **29**, 108–112.
8 T. Gurunathan, S. Mohanty and S. K. Nayak, *Polym.-Plast. Technol. Eng.*, 2016, **55**, 92–117.
9 C. Gao and D. Yan, *Prog. Polym. Sci.*, 2004, **29**, 183–275.
10 B. Voit, *J. Polym. Sci., Part A: Polym. Chem.*, 2005, **43**, 2679–2699.
11 H. Mahdavi and M. T. Hosseinzadeh, *J. Iran. Chem. Soc.*, 2015, **12**, 1465–1472.
12 K. N. Han, B. Y. Yu and S.-Y. Kwak, *J. Membr. Sci.*, 2012, **396**, 83–91.
13 V. Vatanpour, S. S. Madaeni, R. Moradian, S. Zinadini and B. Astinchap, *Separ. Purif. Technol.*, 2012, **90**, 69–82.
14 Y. T. Chung, E. Mahmoudi, A. W. Mohammad, A. Benamor, D. Johnson and N. Hilal, *Desalination*, 2017, **402**, 123–132.
15 S. Afkham, A. Aroujalian and A. Raisi, *RSC Adv.*, 2016, **6**, 108113–108124.
16 S. Prabhu and E. K. Poulose, *Int. Nano Lett.*, 2012, **2**, 32.
17 A. Haider and I.-K. Kang, *Adv. Mater. Sci. Eng.*, 2015, 2015.
18 Y. Sun, B. Mayers and Y. Xia, *Nano Lett.*, 2003, **3**, 675–679.
19 Y. Hao, J. Gao, Z. Xu, N. Zhang, J. Luo and X. Liu, *New J. Chem.*, 2019, **43**, 2797–2803.
20 S. Zhai, H. Hong, Y. Zhou and D. Yan, *Sci. China Chem.*, 2010, **53**, 1114–1121.

21 Y. Zhang, H. Peng, W. Huang, Y. Zhou, X. Zhang and D. Yan, *J. Phys. Chem. C*, 2008, **112**, 2330–2336.
22 K. Maziya, B. C. Dlamini and S. P. Malinga, *React. Funct. Polym.*, 2020, **148**, 104494.
23 M. A. Elrehim, S. Said, A. Ghoneim and G. Turky, *Macromol. Symp.*, 2007, **254**, 1–8.
24 A. Ghanem, A. El-Gendi, M. A. Rehim and K. El-Khatib, *RSC Adv.*, 2016, **6**, 32245–32257.
25 M. A. Yassin, T. A. Elkhooly, S. M. Elsherbiny, F. M. Reicha and A. A. Shokeir, *Heliyon*, 2019, **5**, e02986.
26 A. Slistan-Grijalva, R. Herrera-Urbina, J. F. Rivas-Silva, M. Ávalos-Borja, F. F. Castillón-Barraza and A. Posada-Amarillas, *Phys. E*, 2005, **25**, 438–448.
27 Q. Bao, D. Zhang and P. Qi, *J. Colloid Interface Sci.*, 2011, **360**, 463–470.
28 W. Guo, W.-T. Leu and S.-H. Hsiao, *J. Polym. Res.*, 2007, **14**, 359–372.
29 W. S. Han, *Polym. Compos.*, 2018, **39**, 1967–1977.
30 M. Toroghi, A. Raisi and A. Aroujalian, *Polym. Adv. Technol.*, 2014, **25**, 711–722.
31 G. V. Vimbela, S. M. Ngo, C. Fraze, L. Yang and D. A. Stout, *Int. J. Nanomed.*, 2017, **12**, 3941.